

UNCLASSIFIED

AD 274 217

*Reproduced
by the*

**ARMED SERVICES TECHNICAL INFORMATION AGENCY
ARLINGTON HALL STATION
ARLINGTON 12, VIRGINIA**



UNCLASSIFIED

NOTICE: When government or other drawings, specifications or other data are used for any purpose other than in connection with a definitely related government procurement operation, the U. S. Government thereby incurs no responsibility, nor any obligation whatsoever; and the fact that the Government may have formulated, furnished, or in any way supplied the said drawings, specifications, or other data is not to be regarded by implication or otherwise as in any manner licensing the holder or any other person or corporation, or conveying any rights or permission to manufacture, use or sell any patented invention that may in any way be related thereto.

274 217

TECHNICAL INFORMATION SERIES

AD
ASTIA

AN INVESTIGATION OF THE PROPERTIES
OF A REPETITIVELY FIRED TWO-STAGE
COAXIAL PLASMA ENGINE

FILE COPY

Return to

ASTIA

ARLINGTON HALL STATION

ARLINGTON 12, VIRGINIA

Attn: TIRS

(5)

SPACE SCIENCES LABORATORY

AEROPHYSICS OPERATION

AN INVESTIGATION OF THE PROPERTIES
OF A REPETITIVELY FIRED TWO-STAGE
COAXIAL PLASMA ENGINE

By

Per Gloersen, Bernard Gorowitz, Warren A. Hovis, Jr.
and Richard B. Thomas, Jr.

R62SD28 - Class I
April, 1962

MISSILE AND SPACE VEHICLE DEPARTMENT

GENERAL  ELECTRIC

CONTENTS

PAGE

List of Figures	iii
Abstract	iv
1. <u>Introduction</u>	1
2. <u>Operating Principles</u>	1
2.1. Single Stage Operation	1
2.2. Two-Stage Operation	6
3. <u>External Features of the Two-Stage Pulsed Plasma Engine</u>	8
3.1. Input Voltage Characteristics	8
3.2. Mechanical Characteristics	9
4. <u>Examination of the Species Present in the Plasma</u>	10
4.1. The Necessity for Detailed Measurements	10
4.2. Spectrographic Measurements	11
4.3. Photoelectric Spectral Mapping	12
4.4. Pulse Sampling Technique	12
5. <u>Concluding Remarks</u>	14
References	15

LIST OF FIGURES

PAGE

1. Two-Stage Plasma Gun Configurations	16
2. Vacuum Test Chamber	17
3. Approximate Pressure Distribution in the Two-Stage Coaxial Gun	18
4. Oscillograph Tracings of Voltage Waveforms from the First and Second Stages of the Two-Stage Pulsed Plasma Engine	19
5. Interstage Delay Time Measurements	20
6. Expanded Trace of the Voltage Waveform from the Second Stage of the Two-Stage Pulsed Plasma Engine	21

ABSTRACT

A repetitively fired two-stage coaxial plasma engine ~~was~~^{was} successfully operated in a 3 x 13 ~~cm~~^{cm} test chamber under conditions closely simulating those of outer space, that is, with negligible interaction between the plasma exhaust and the residual gas in the test chamber. ~~The operating principles of the two-stage engine will be described in detail, along with the advantages obtained with a two-stage approach.~~ Results of some preliminary measurements of pressure distribution in the engine, thrust, specific impulse, input mass flow, and energy efficiency ~~will be~~^{are} presented. ~~A~~^{was}, a photoelectric spectrum mapping technique ~~has~~^{has} been developed which takes advantage of the repetitive nature of the pulsed plasma exhaust. ~~The arrangement consists of a 500 mm Ebert scanning monochromator with curved slits, a photomultiplier detector and integrating amplifier, and a strip chart recorder on which the spectra are printed.~~ This technique ~~has been~~^{was} used to obtain emission spectra from various points inside and beyond the muzzle of the two-stage gun, and ~~has been~~^{was} successful in yielding many more spectral lines than the standard photographic technique, ~~to which it will be compared. Generally, the results have been~~^{some} ~~that~~^{only} argon ion and oxygen ion lines appear in all parts of the gun and in the exhaust. ~~Most notable in their absence are the~~^{///} copper and silicon ion lines, which ~~was~~^{///} appeared in the exhaust of an earlier single-stage self-triggered coaxial gun, and which indicate erosion of the electrodes and insulators, ~~respectively,~~^{were absent.} A detailed discussion of these and additional spectral results will be given.

1. Introduction

This paper will describe the operating principles of a two-stage repetitively fired coaxial plasma engine and some preliminary detailed plasma diagnostics on the excited engine propellant in various locations inside and outside the second stage coaxial gun. It should be mentioned in advance that while some mechanical measurements have been made on this device which have proven to be most encouraging, the detailed mechanism for the acceleration of the plasma is not well understood; only partially verified theoretical models exist at this time. Thus, the diagnostic data to be presented here represents but a beginning towards a more complete understanding of coaxial gun operation.

2. Operating Principles

2.1 Single Stage Operation

Since the operation of the second stage of our two-stage device is similar to that of a simple coaxial gun with pulsed gas feed, it might be well to make a few remarks on the theory of its operation before we proceed with the discussion of the two-stage device.

Consider an element of volume at a point (z, r) at a particular time t . Here we use cylindrical coordinates to describe the space contained between two coaxial conducting cylinders of radius a and b respectively. Let $\rho(z, r)$ be the gas density within the gun. Then if we consider the force balance in the z direction, Newton's second law allows us to write:

$$P(z, r) - P(z + \Delta z, r) = \frac{d}{dt} \left\{ \rho(z, r) \Delta z \frac{dz}{dt} \right\} \quad (1)$$

where $P(z, r)$ is the pressure in the gas at a point (z, r) . If we expand the left-hand side and perform the derivative operation on the right

$$-\frac{\partial P}{\partial z}(z, r) = \frac{d\rho}{dt}(z, r) \frac{dz}{dt} + \rho(z, r) \frac{d^2 z}{dt^2}. \quad (2)$$

Now the density depends only implicitly upon the time through the coordinates so that

$$\frac{d\rho}{dt} = \frac{\partial \rho}{\partial z} \frac{dz}{dt} + \frac{\partial \rho}{\partial r} \frac{dr}{dt}, \quad (3)$$

since the axial symmetry excludes any dependence upon angle. If we assume that mass movement in the radial direction can be neglected, Equation (3) can be used to write Equation (2) as

$$-\frac{\partial P}{\partial z} = \frac{\partial \rho}{\partial z} \left(\frac{dz}{dt} \right)^2 + \rho(z, r) \frac{d^2 z}{dt^2}. \quad (4)$$

If the only important part of P is the magnetic pressure given by

$$P = -\frac{1}{2\mu_0} B^2(z, r) + \text{constant},$$

then Equation (4) becomes

$$\frac{B(r, z)}{\mu_0} \frac{\partial B}{\partial z} = \frac{\partial \rho}{\partial z} \left(\frac{dz}{dt} \right)^2 + \rho(z, r) \frac{d^2 z}{dt^2}. \quad (5)$$

With appropriate approximations, the results of several simple models can be obtained from Equation (5). For example, the mass slug model (Refs. 1, 2 and 3), where the magnetic field is entirely excluded from the mass of plasma and ρ is taken constant over a length l , we obtain by integrating Equation (5) over both r and z

$$\int_a^b \frac{B^2 2\pi r dr}{2\mu_o} = \pi (b^2 - a^2) l \rho \frac{d^2 z}{dt^2} \quad (6)$$

The magnetic field can be calculated and is just $B_{\Theta} = \frac{\mu_o i}{2\pi r}$, which enables us to integrate Equation (6) to obtain

$$\frac{\mu_o}{4\pi} i^2 \ln \frac{b}{a} = \frac{i^2 L'}{2} = \pi (b^2 - a^2) l \rho \frac{d^2 z}{dt^2}, \quad (7)$$

where L' is the inductance per unit length of a pair of coaxial cylinders. As has been indicated previously (Refs. 4 and 5), this model does not lend itself to a comparison with experiment because (1) the plasma is not rigid and (2) the force is a strongly varying function of the radius, causing a slip of adjacent ring elements of plasma by one another. With Equation (5) as a basis, it is possible to introduce several refinements which greatly improve upon the slug model.

Where the gas density is not constant or where mass is accumulated in the current sheet, its distribution might be expressed in the form of a power series

$$\rho(z, r) = \sum_{i=0}^n \rho_i(r) z^i \quad (8)$$

If ρ_0 is small and ρ_1 is positive, and if we neglect terms of order two or higher, we have the snow plow model (mass accumulation in the current sheet) as expressed by Hart (Ref. 2). It is interesting to note that a current sheet proceeding into a gas sample with linearly decreasing density, but with no mass accumulation, has much the same form (ρ_1 is negative).

In either case, Equation (5) takes the form

$$\frac{B(r, z)}{\mu_0} \frac{\partial B}{\partial z} = \rho_1 \left(\frac{dz}{dt} \right)^2 + (\rho_0 + \rho_1 z) \frac{d^2 z}{dt^2} \quad (9)$$

which is usually averaged in the radial direction by neglecting the dependence of the various terms on r .

This, of course, is not at all necessary, and it might be useful to consider the radial dependence here also. It may well be necessary, also, to include higher order terms in the expansion of $\rho(r, z)$ in order to obtain agreement with experiment.

Another feature of the usual treatment (Refs. 2 and 3) of the snowplow and slug models that does not permit reasonable comparison with experiment is that no allowance is made for transmitting mass through the current sheet. Hart has proposed an alternative fate for some of the accumulated mass in the snowplow model. He has arbitrarily assumed that half of the accumulated mass goes into random rather than directed motion. While it is probably true that the propellant is heated to some extent in the acceleration process, the extreme suggested by Hart would appear appropriate only in the case of pressure-driven shock waves. A more desirable approach might be to assign an arbitrary fraction to the amount of propellant heated, the value being left to empirical determination.

A more realistic model, at least for the low density region of operation, has been proposed by Lovberg and his co-workers (Refs. 6, 7 and 8). It presumes mass leakage through the current sheet. In fact, for the case of complete sheet transparency, the continuity relations can be used (Ref. 5)

to obtain velocity and density profiles behind the current sheet:

$$v_i(r) \approx \frac{\mu_o i^2}{8\pi^2 r^2 \rho_i v_s} \quad (10)$$

$$\rho_2(r) \approx \frac{\rho_1}{1 - \mu_o i^2 / 8\pi^2 r^2 \rho_1 v_s^2} \quad (11)$$

where v_s and v_i are the velocities of the current sheet and the mass flow behind the sheet, respectively; i is the total current; and ρ_1 and ρ_2 are the densities ahead of and behind the sheet, respectively. Thus, if one assumes that the experimentally observed flatness of the current sheet (Refs. 6, 7 and 8) (v_s independent of r) is a fundamental property of such devices, and that the initial density is uniform, the radial dependences of v_i and ρ_2 assume the particularly simple forms given by the explicit appearance of r in Equations (10) and (11).

In Equations (10) and (11) it has been assumed that the density is sufficiently low that ion-neutral collisions can be neglected, and that the temperatures ahead of and behind the current sheet are the same. At intermediate densities it will be necessary to take such collisions into account by assuming some degree of heating, but less than that expected on the basis of a pressure-driven shock wave. At still higher densities, the current sheet may no longer be able to precede the accelerated propellant flow due to prohibitively short ion-electron recombination times at room temperatures. Before one ventures further into theoretical models in this regime, it would be well to obtain some good experimental data on which to base such models.

When operating a single stage coaxial gun, there is the choice of several modes of operation: pulsed or steady propellant feed and self-triggered or delayed externally switched electrical energy feed. The four permutations permitted by the listed variables each have their own disadvantages. The two permutations involving external switching may give rise to an unsolvable practical problem of designing a high-power switch with a reasonable weight capable of repetitive operation. With self-triggering, the problem is premature breakdown either at too low a density during propellant entry or too low a voltage during the charging of the energy storage capacitor, depending on whether the propellant feed is pulsed or steady. Such premature breakdowns give rise to poor mass utilization or poor magneto-plasma coupling, respectively.

One possible way out of this dilemma is to choose a sufficiently high repetition rate so that a lightweight pulse-forming network can be used to supply electrical energy to the propellant in the form of square waves, or some reasonable approximation thereto. We have chosen still another way which may lead to greater versatility in pulsing rates, viz. the two-stage approach, which at least in principle supplies propellant to the second stage in a sharply rising pressure front.

2.2 Two-Stage Operation

As in single stage operation, one has the choice of both pulsed and steady propellant feed in two-stage operation. While pulsed propellant feed may offer some advantages in refining the operation of our two-stage plasma engine, the device apparently works properly in a limited range of

densities with steady propellant feed. We have therefore chosen the latter alternative for our initial studies due to its inherent simplicity.

The electrode configurations used in these studies are shown in Figure 1. The muzzle of the plasma engine was inserted into a 3' x 13' vacuum test chamber (Figure 2), which could be maintained at a pressure of 10^{-5} mm while flowing in propellant (usually argon) at the rate of 10^{-3} g/sec. In the top configuration (Figure 1) there is a gas flow regulator ahead of the small inlet tube to the first stage. The gas enters the first stage, in this case a T-tube, through a hole in one of the T-tube electrodes. The gas enters the second stage radially through small interstage holes.

Figure 3 shows the approximate distribution of pressures in the experimental arrangements with a steady mass flow of about one milligram of argon per second. The plenum pressure was about 5 mm, as measured by a dial gauge. The testing tank pressure of 10^{-5} mm was determined with a Phillips ionization gauge. This residual gas pressure is consistent with the mass flow rate and the rated combined pumping speeds of the three 32" oil diffusion pumps evacuating the test chamber. The pressure distribution in the second stage was estimated by a consideration of the pumping speed of the gun cylinder, the flow rate, and the muzzle pressure. The approximate first stage pressure was determined by measuring the minimum breakdown potential and considering the Paschen curve for argon. The estimated steep pressure drops result from the interstage constrictions. With this distribution of pressures it was found that the first stage could be fired at will through an external switch at low power. The second stage, on the other

hand, which is directly connected to the energy storage capacitor, can support potentials at least up to 15 KV.

In operation, the firing of the first stage gives rise to a pressure pulse of sufficient magnitude that breakdown occurs when it is transferred to the second stage. It may well be that the transfer of partially ionized gas or metastables from the first to the second stage assists in the second stage breakdown. Another possibility that cannot be completely ruled out at this point is that the second stage discharge may be triggered by photons produced in the first stage. This latter possibility is not consistent, however, with the observation of measurable and variable interstage delay times with the second configuration shown (Figure 1), where second stage gas is exposed to first stage photons from the beginning of first stage breakdown.

3. External Features of the Two-Stage Pulsed Plasma Engine.

3.1 Input Voltage Characteristics

In Figure 4 are shown voltage waveforms from the first and second stages. It can be seen that the second stage (bottom trace) fires in perfect synchronization with the first stage (top trace). The interstage delay time cannot be seen on the time scale shown in Figure 4 but has been measured on expanded traces. The results of such measurements are shown in Figure 5. The curves shown here are all for a constant mass flow of 1 mg of argon/sec. In all cases, it can be seen that the interstage delay becomes less as more energy is provided to the first stage, presumably because the shock-heated gas reaches the interstage ports more quickly at higher first stage energies. The first curve on the left is for a T-tube without a backstrap.

The second curve is for a T-tube with a backstrap. The third curve, consisting of a triaxial arrangement of electrodes, is for a first stage configuration not shown in Figure 1. It can be seen that the second stage potential was not critical in determining interstage delay times in the range 5-11 KV.

In Figure 6 is shown an expanded trace of the voltage waveform from the second stage. The fact that the waveform is nearly critically damped implies that most of the electrical energy is deposited in the plasma in the first quarter cycle of the discharge. Since the time scale in Figure 6 is 10 microseconds/cm, the energy deposition apparently takes place in less than 5 microseconds.

3.2 Mechanical Characteristics

At this early stage of the game we have not yet made careful measurements of the thrust and specific impulse over wide ranges of operating conditions. Rather, we have concentrated on exploring the details of operation in order to possibly refine the configuration before going to more detailed mechanical measurements. In order to establish some idea of how well the two-stage engine works, some measurements were made of thrust and specific impulse delivered by the preliminary configuration for just one power and mass flow input.

The thrust was measured by the simple pendulum technique, that is, by allowing the engine exhaust to strike the pendulum in the vacuum test chamber, held at 10^{-5} mm. Of course this method gives but a crude estimate of thrust, but the result was 0.02 lb. thrust for an average power input of 7 kilowatts. The pulsing rate was 20 per second, and the natural frequency

of the pendulum was sufficiently low that the pendulum assumed a steady deflection during the run. More careful and extensive studies on a suitable thrust stand are in the planning stage.

The specific impulse has been measured in several ways: by streak camera records of the luminous front beyond the muzzle, by two-station photomultiplier telescope measurements of time-of-flight of the luminous pulse between the breach and muzzle of the gun, and finally by time-of-flight of individual species in and beyond the gun barrel. The agreement between the data obtained by the various methods was within experimental error. Under the same conditions used to obtain the .02 lb. thrust, the specific impulse was found to be 5000 seconds, corresponding to a power conversion efficiency of 32%. At higher operating voltages, specific impulses as high as 9000 seconds have been observed. These figures also correspond to an exhaust mass flow rate of about one milligram/second, which, probably strictly as a matter of coincidence, happened to be the measured input mass flow rate.

4. Examination of the Species Present in the Plasma.

4.1 The Necessity for Detailed Measurements

The operating characteristics of the two-stage accelerator as presented so far here are far from complete. Aside from measuring the gross mechanical properties in more detail as outlined above, it is very desirable to obtain an explicit, rather than implicit measure of mass flow rate in the exhaust so that mass utilization may be determined directly rather than inferred. Also, it is almost certain that the numerous species in the

exhaust have a spread of directed velocities rather than just one, as inferred from the measurements above. An indication of this situation is the fact that the photomultiplier telescope records of the light pulses emanating from the muzzle indicate pulse widths of 20-30 microseconds, compared with the 5 microsecond time required to deposit the electrical energy. The measurements to be presented below represent a start in the right direction towards obtaining such detailed results. We shall describe both photographic mapping of the spectra emitted by the luminous gun plasma, and some preliminary time-of-flight data for individual luminous species obtained by a photoelectric pulse-sampling technique (Ref. 9).

4.2 Spectrographic Measurements

A 1.5 meter concave grating instrument was used to obtain spectrograms of the gun plasma both at the breech and the muzzle. Since the luminosity was rather weak, long exposures during repetitive operation were required in order to obtain even the few lines observed. At both locations most of the lines recorded were due to argon ions. A few oxygen ion lines were also present. Notable in their absence were silicon ion lines, indicative of low insulator erosion rates, copper ion lines, indicative of low electrode erosion, and argon atom lines, showing that electron-ion recombination rates must have been low in the regions investigated.

We were unable to obtain spectrograms 5 cm or more beyond the muzzle since the luminosity was much too weak there.

4.3 Photoelectric Spectral Mapping

A 500 mm Ebert scanning monochromator with a photomultiplier detector and signal integrator was used to record on a strip chart the spectra emitted by the luminous plasma at various points inside and exterior to the gun. At least an order of magnitude increase in sensitivity was realized with this technique, resulting in the observation of many more lines than obtained photographically. The conclusions remain essentially the same as those reached with the photographic measurements, only with more emphasis. The only additional lines observed were due to cyanogen and carbon, and then only near the beginning of a run, while the gun was "cleaning up".

In spite of the vastly increased sensitivity, we were again unable to find argon emission spectra 5 cm or more beyond the muzzle. A very weak carbon line was occasionally observed beyond the muzzle, leading to speculation that the "cold" plasma emanating from the gun was colliding with residual oil vapor in the test chamber.

4.4 Pulse Sampling Technique

The repetitive nature of the engine allows the use of time resolved studies with gated photomultipliers, where portions of the signal from 0.1 μ sec to several microseconds in width may be observed. Time averaging of the signal by the use of long time constants and location of the gate at successive intervals in time throughout the light signal give an accurate time profile of the emitted light. The pulsed nature of the photomultiplier can be utilized to produce higher gains than possible with steady operation and a higher signal to noise ratio (Ref 10).

Such a pulse sampling technique was applied to our photoelectric spectral measurements by using a gated photomultiplier tube, with considerable increase in the sensitivity compared even with the integrator technique discussed in the previous section. The details of this technique have been described elsewhere (Ref. 9).

With this arrangement we were able to determine the average time of arrival of argon ions at the muzzle of the gun, relative to the initiation of the first stage discharge. Since the interstage delay times could be observed on the oscilloscope monitoring first and second stage voltage waveforms, these were subtracted from the pulse dissector delay settings to obtain breech-to-muzzle time-of-flights. Using the peak of the pulse as the fiducial mark, the specific impulses as obtained from the argon ion were comparable with the earlier results. Pulse widths were only 2 or 3 microseconds, in sharp contrast to the 20 microsecond or so widths observed with the total light, but more in accordance with the time in which the electrical energy is deposited in the plasma. The pulse rose very sharply, with a more slowly decaying tail, giving the impression of a rather narrow range of argon ion velocities emanating from the gun.

In spite of the additional increase in sensitivity realized by the present recording technique, we were still unable to find emission spectra other than an occasional carbon line 5 cm or more beyond the muzzle when using argon as a propellant. Upon switching to helium as a propellant, however, we were able to detect emission spectra at least 25 cm away from the muzzle. We chose the helium atom 3888A line for further study. Not enough data were

available at this writing to draw definite conclusions, but qualitatively it appeared as if the pulse widths were about the same as at the muzzle, and the pulses had slowed down somewhat after leaving the gun. The specific impulse observed was the same as for argon, but that is not surprising in view of the fact that the mass flow of helium had to be made equal to that used with argon in order to obtain reliable operation of the gun in the steady propellant feed mode with this particular electrode configuration.

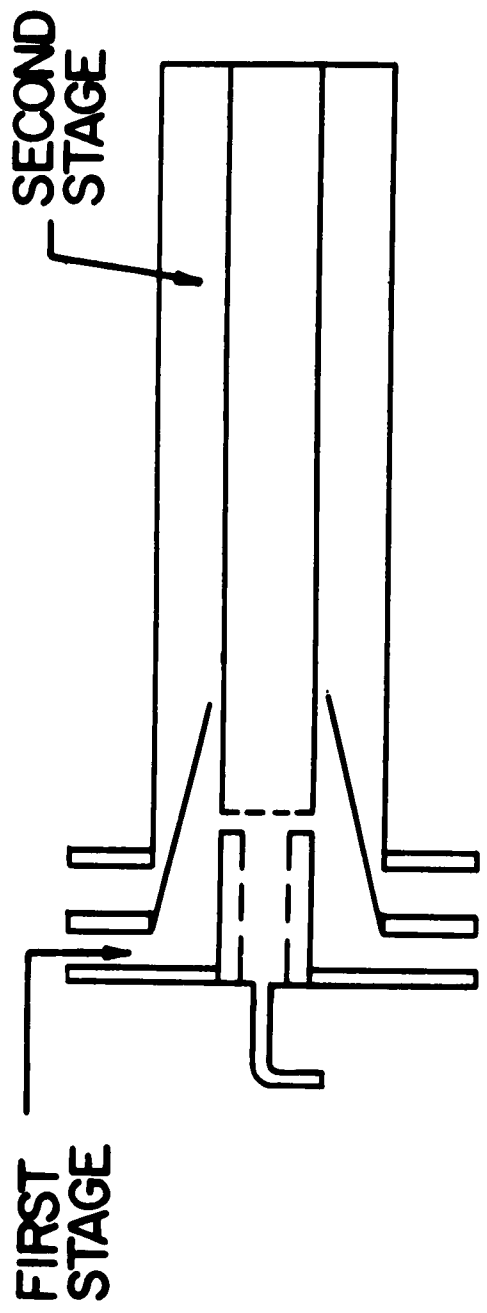
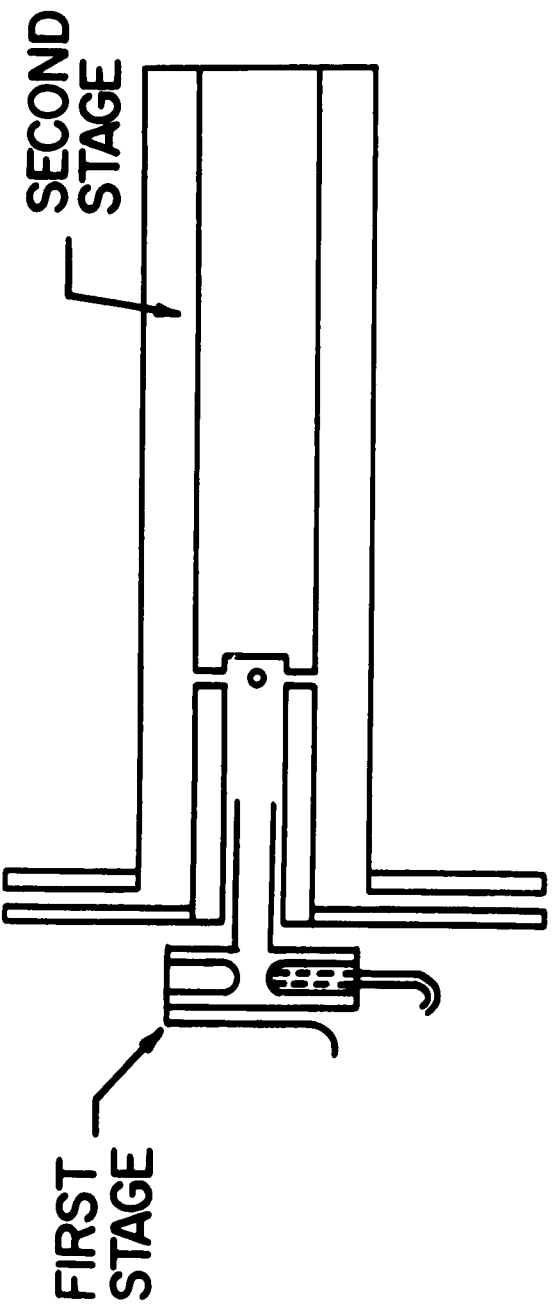
5. Concluding Remarks

As should be readily apparent by now, this paper has been of the nature of a progress report on a program which is just beginning, involving detailed diagnostic studies of the operation of a two-stage pulsed plasma engine. Refinements in the design of the gun, not apparent from the early mechanical measurements, have already been indicated by such detailed diagnostics. We hope to have in operation very shortly a method of detecting non-luminous species in the exhaust by absorption spectroscopy.

In summary, then, we have accomplished the following: We have measured the thrust, specific impulse, and energy efficiency at one particular operating point (7 Kw input power, 10^{-3} gm/sec mass flow). We have measured specific impulse at two other operating points, making the range of observed specific impulse thus far 5,000 - 9,000 seconds. We have used three different spectrometric techniques, each new one with increasing sensitivity, to obtain identification of species in the gun plasma. Finally, we have used a special pulse sampling technique to obtain preliminary information on time-of-flight and velocity spread of individual species in the gun plasma.

REFERENCES

1. John Marshall, Jr., "Performance of a Hydromagnetic Plasma Gun", *Phys. Fluids* 3, 134 (1960)
2. Philip J. Hart, "Plasma Acceleration with Coaxial Electrodes", *Phys. Fluids* 5, 38 (January 1962)
3. Philip M. Mostov, Joseph L. Neuringer, and Donald S. Rigney, "Electromagnetic Acceleration of a Plasma Slug", *Phys. Fluids* 4, 1097 (1961)
4. J. C. Keck, F. Fishman, and H. E. Petschek, "Experimental Study of the Flow Field in a MAST of Large Radius Ratio", *Bul. Am. Phys. Soc. II*, 6, 278 (1961)
5. Per Gloersen, "Pulsed Plasma Accelerators", ARS Paper No 2129-61, read at the ARS Space Flight Report to the Nation in New York (October 1961)
6. R. H. Lovberg, "The Magnetic Acceleration of a Plasma", Paper G-3 at the Gatlinburg Meeting of the Division of Plasma Physics (APS), November 1960
7. L. C. Burkhardt and R. H. Lovberg, "The Current Sheet in a Coaxial Plasma Gun", to be published.
8. B. R. Hayworth and R. H. Lovberg, "Measurements of Ion Momentum Transfer in a Coaxial Plasma Gun", *Bul. Am. Phys. Soc. II*, 7, 142 (1962)
9. W. A. Hovis, Jr., "Time-Resolved Studies of Fast Decay Times", *Bul. Am. Phys. Soc. II*, 7, 157 (1962); to be published in *J. Opt. Soc. Am.*
10. C. F. Hendee and W. B. Brown, "Stroboscopic Operation of Photomultiplier Tubes", *Philips Technical Review* 19, 50 (1957)



TWO-STAGE PLASMA GUN CONFIGURATIONS

Figure 1.

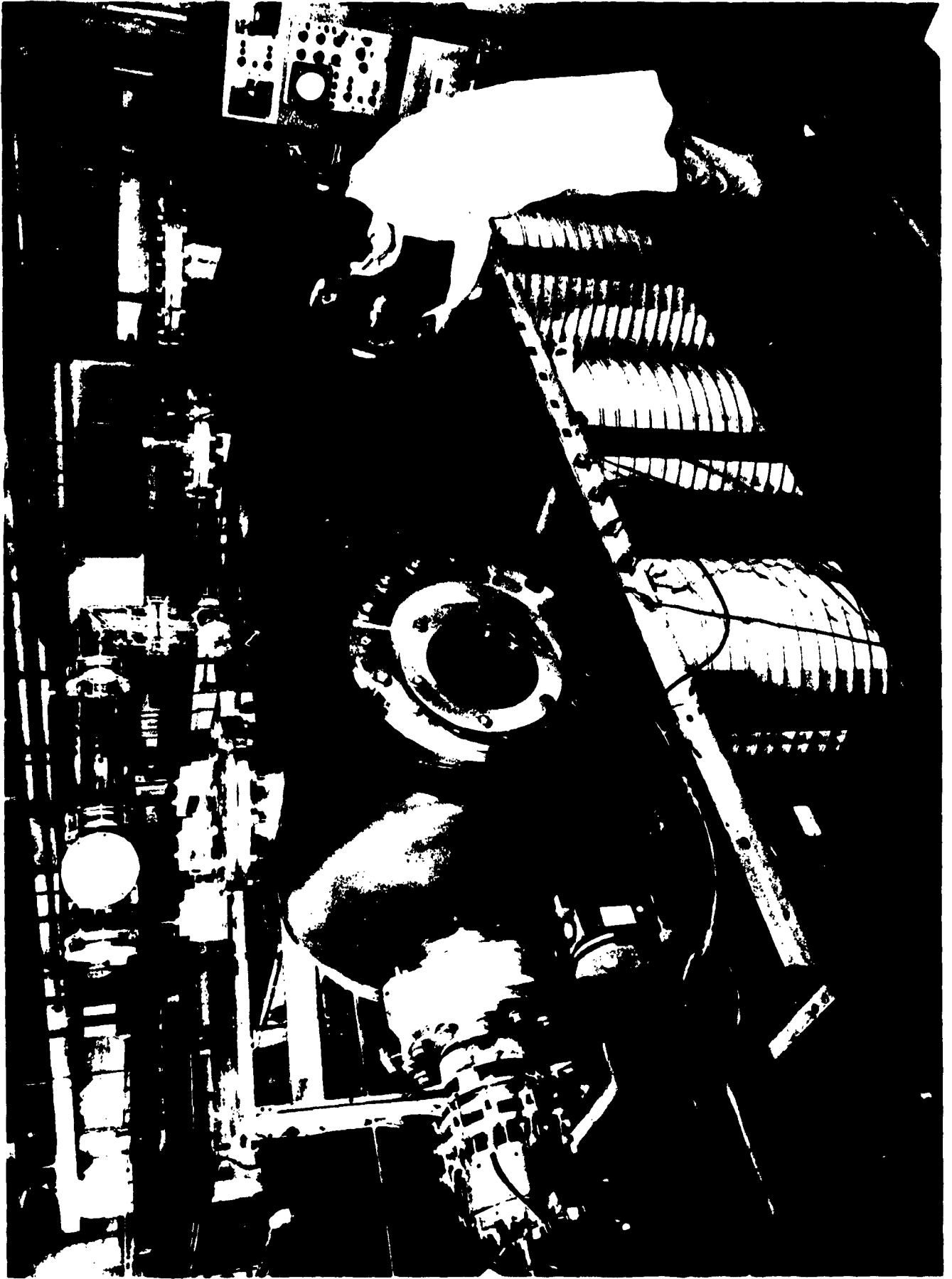


Figure 2. Vacuum Test Chamber.

APPROXIMATE PRESSURE DISTRIBUTION IN THE TWO-STAGE COAXIAL GUN

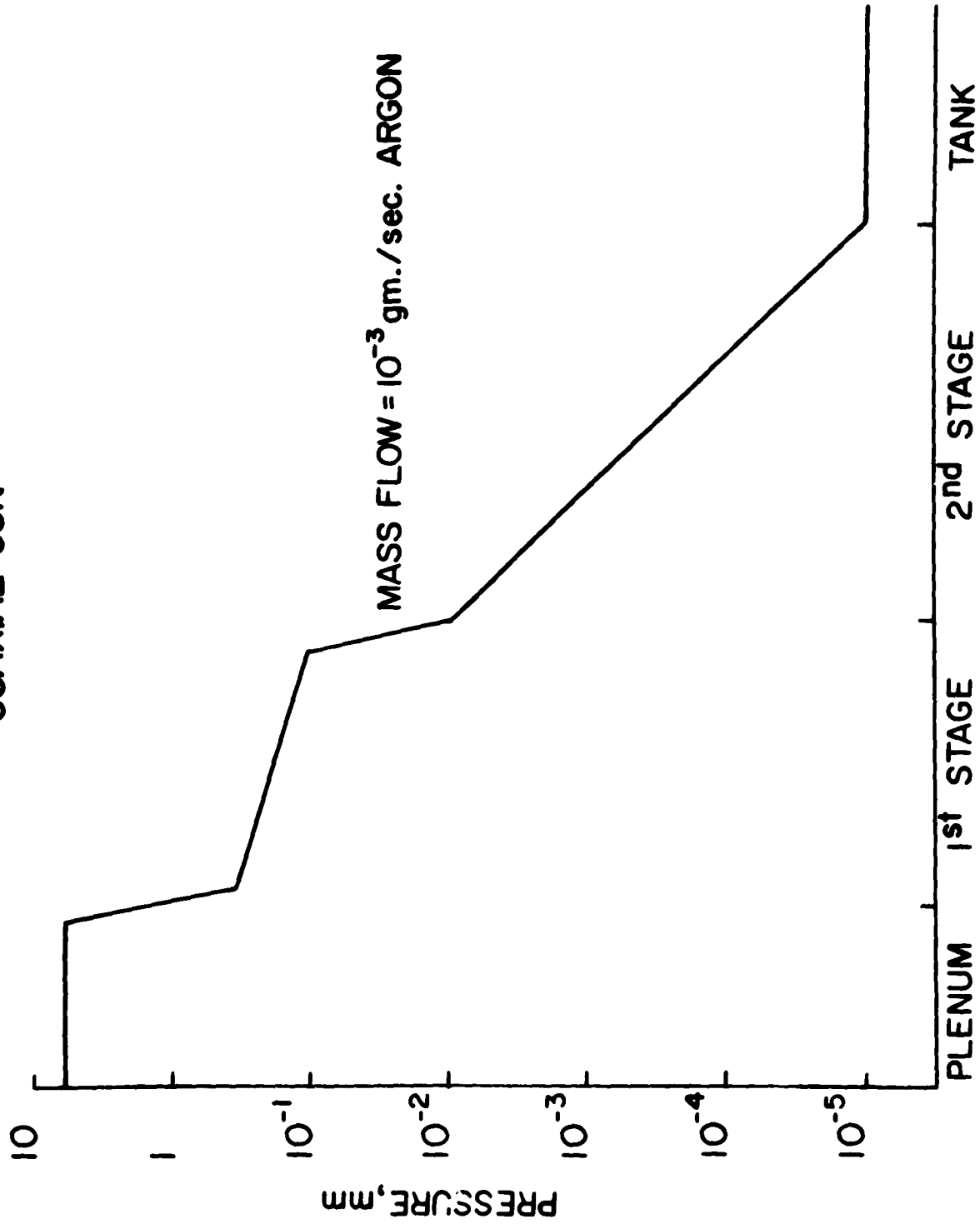


Figure 3.

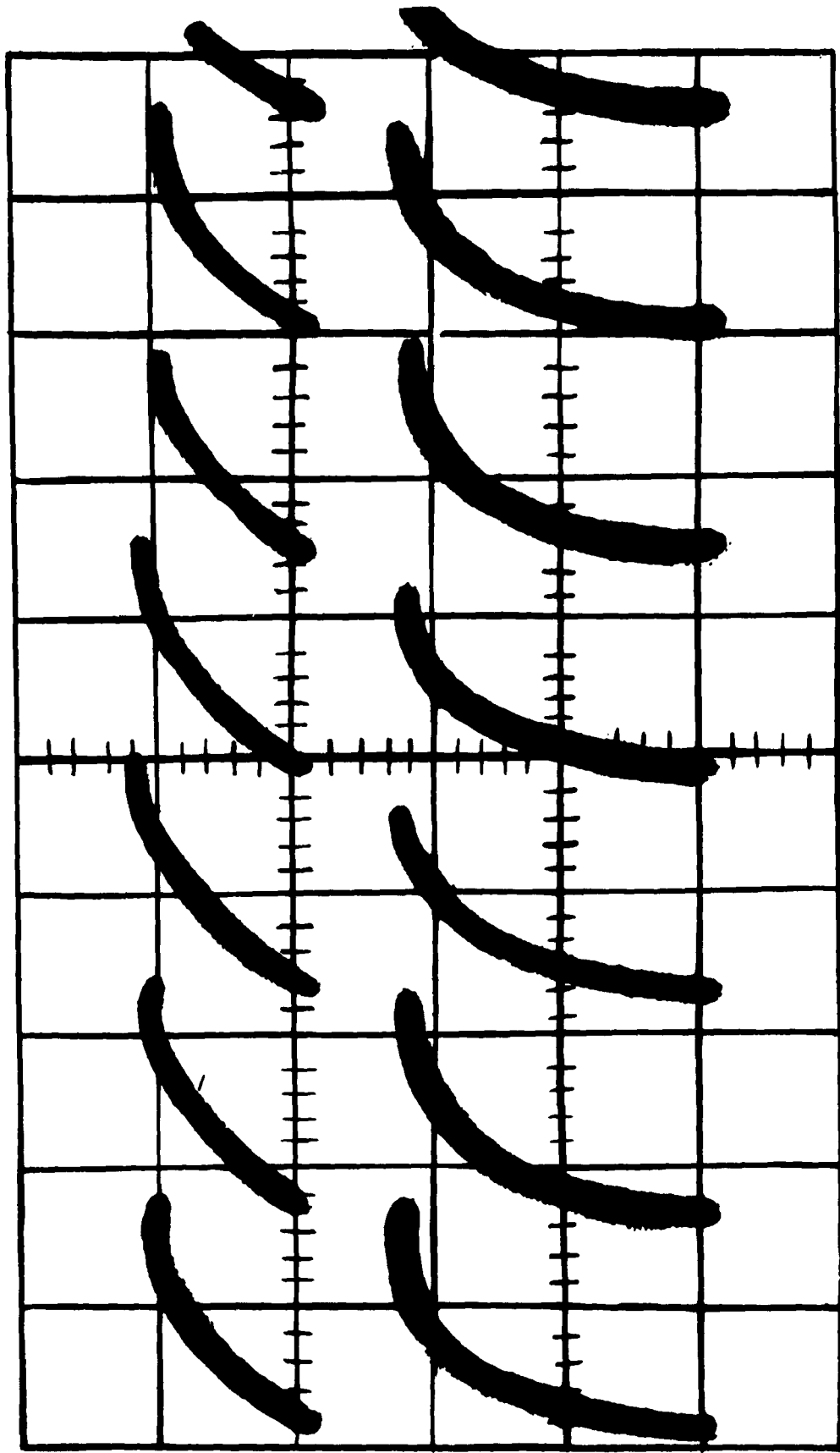


Figure 4. Oscilloscope Tracings of Voltage Waveforms from the First (Top Trace) and Second (Bottom Trace) Stages of the Two-Stage Pulsed Plasma Engine.

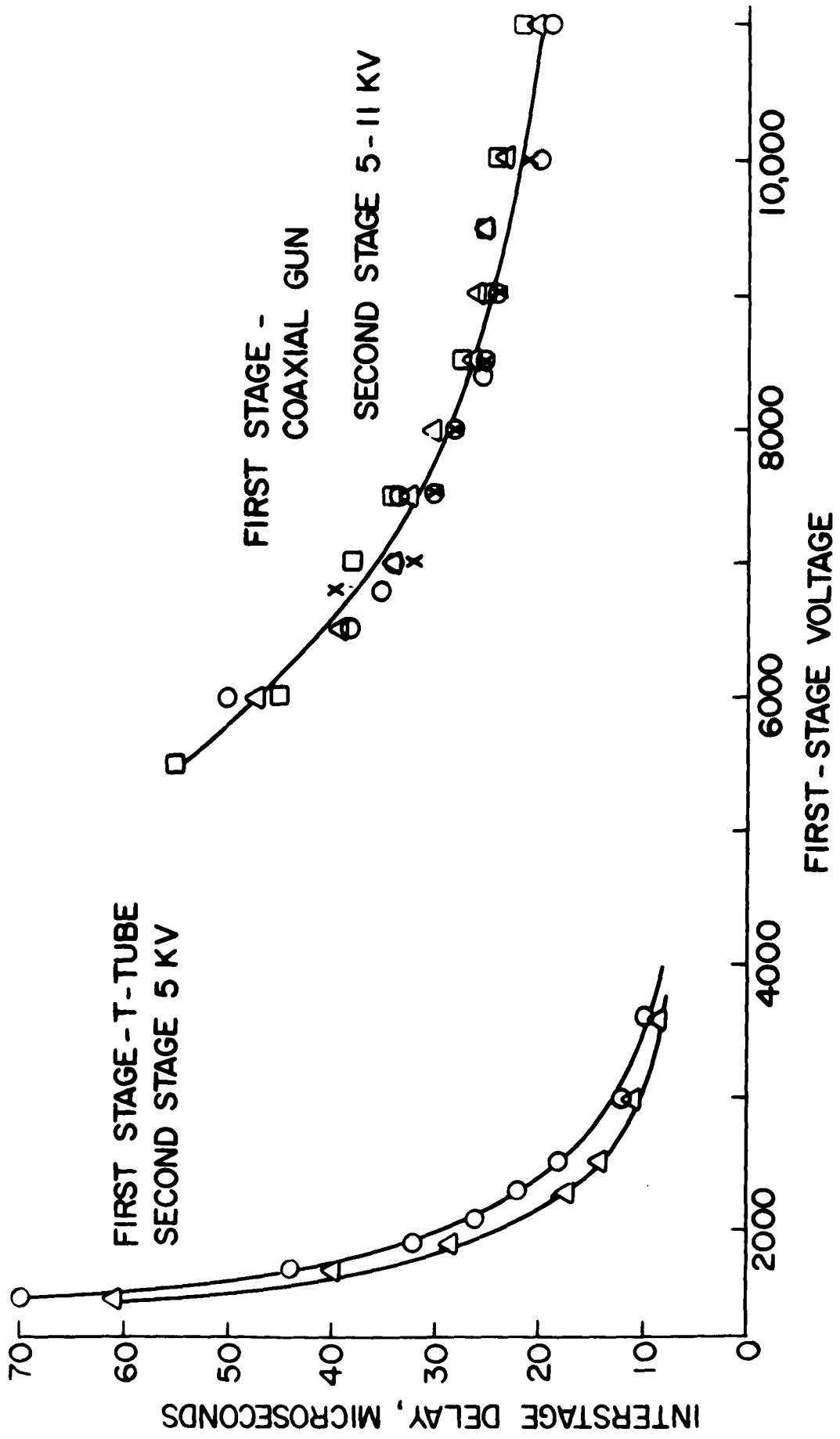


Figure 5. Interstage Delay Time Measurements.

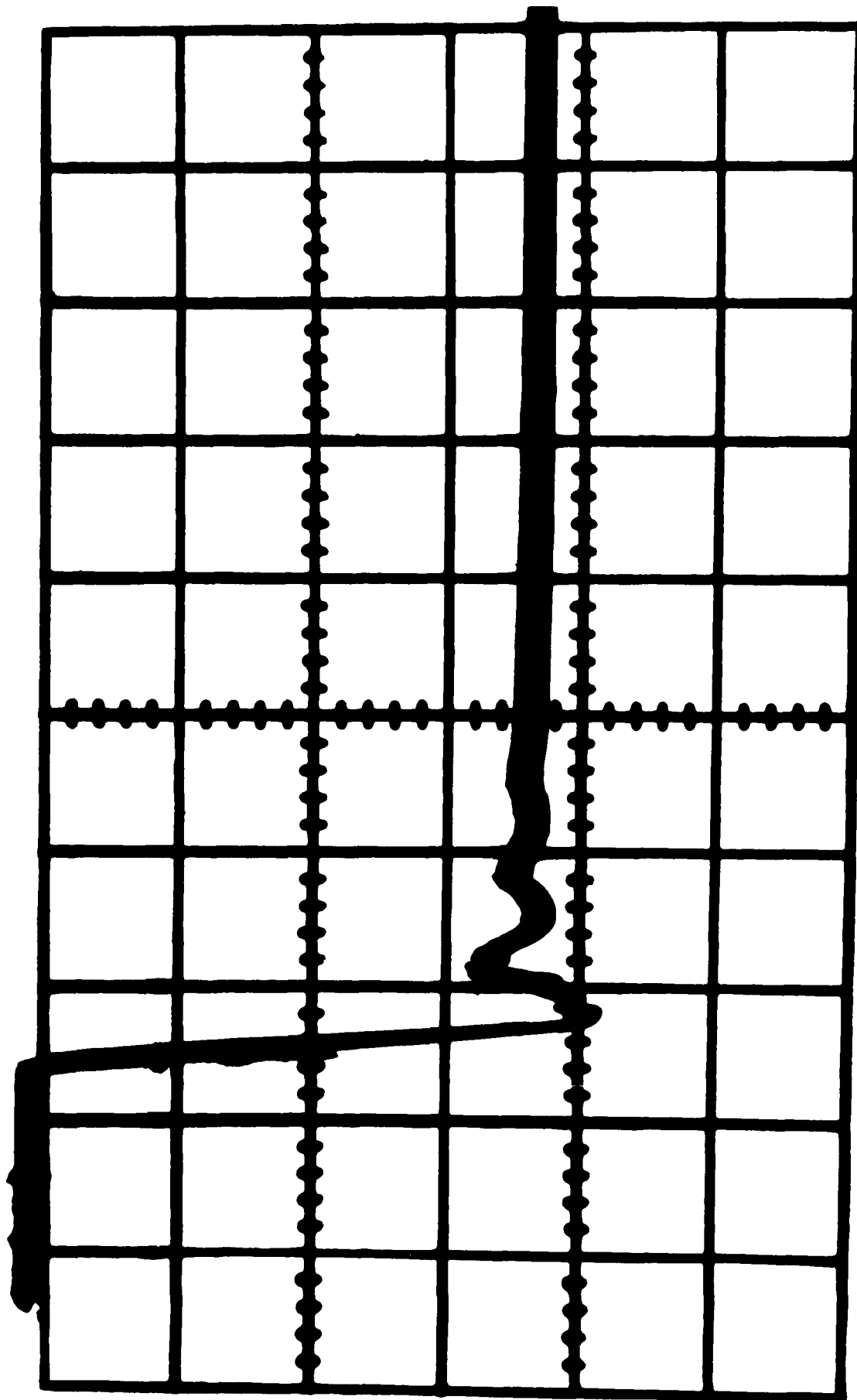


Figure 6. Expanded Trace of the Voltage Waveform from the Second Stage of the Two-Stage Pulsed Plasma Engine.

SPACE SCIENCES LABORATORY
MISSILE AND SPACE VEHICLE DEPARTMENT

TECHNICAL INFORMATION SERIES

AUTHOR P. Gloersen, et. al.	SUBJECT CLASSIFICATION PLASMA PHYSICS	NO. R62SD28 DATE April 1962
TITLE AN INVESTIGATION OF THE PROPERTIES OF A REPETITIVELY FIRED TWO-STAGE COAXIAL PLASMA ENGINE		
ABSTRACT A repetitively fired two-stage coaxial plasma engine has been successfully operated in a 3 x 13 foot test chamber under conditions closely simulating those of outer space, that is, with negligible interaction between the plasma exhaust and the residual gas in the test chamber. The operating principles of the two-stage		
G. E. CLASS I	REPRODUCIBLE COPY FILED AT G. E. TECHNICAL INFORMATION CENTER 3198 CHESTNUT STREET PHILADELPHIA, PENNA.	NO. PAGES 21
GOV. CLASS None		
engine are described in detail, along with the advantages obtained with a two-stage approach. Results of some preliminary measurements of pressure distribution in the engine, thrust, specific impulse, input mass flow, and energy efficiency are presented. In addition, a photoelectric spectrum mapping technique which takes advantage of the repetitive nature of the pulsed plasma exhaust is described. This technique has been used to obtain emission spectra from various points inside and beyond the muzzle of the two-stage gun, and has been successful in yielding many more spectral lines than the standard photographic technique, to which it is compared. The results have been that only argon ion and oxygen ion lines appear in all parts of the gun and in the exhaust.		

By cutting out this rectangle and folding on the center line, the above information can be fitted into a standard card file.

AUTHOR *P. Gloersen, Norman R. Hunt, Richard B. Thomas, Bernard M. Gray*

COUNTERSIGNED *Joseph Fisher*

DIVISION Defense Electronics

LOCATION Valley Forge Space Technology Center, King of Prussia, Pa.